Hard X-Ray XAFS Beamlines (BL-3, 4 and 5) of SR Center

Misaki Katayama[1] and Yasuhiro Inada[2]

1) Japan Synchrotron Radiation Research Institute, Sayo-cho, Hyogo, 679-5198, Japan
2) College of Life Sciences, Ritsumeikan University, Kusatsu, Shiga, 525-8577, Japan

Abstract

This article summarizes the upgrading of the hard X-ray XAFS beamlines at the SR Center of Ritsumeikan University since 2009. BL-3 is a general-purpose XAFS beamline equipped with a focusing mirror and can be used up to 9 keV. The BL-3 is equipped with a 3-element SSD, and the measurement by the fluorescence-yield method is possible in addition to the measurement by the transmission method. It is also possible to perform *in-situ* XAFS measurement under a reaction gas atmosphere at elevated temperatures. BL-4 is a non-focusing XAFS beamline which can measure up to about 10 keV, and the imaging XAFS measurement is possible using a two-dimensional detector. It is effective in analyzing the reaction distribution in the plane of a flat sample such as the electrode of a rechargeable battery. BL-5 is a special beamline which uses white X-rays and is equipped with two kinds of time-resolved XAFS instruments with a dispersive X-ray optics. A dispersive XAFS instrument, which simultaneously achieves XAFS measurements at the absorption edge of two elements using two curved crystals at the same time, is useful for analyzing the interelement correlation to the function of the material. The vertically dispersive XAFS instrument using a cylindrically bent crystal is capable of the time-resolved XAFS measurement for one-dimensional region of the sample. It is possible to perform XAFS measurement by simultaneously decomposing time and space for the phenomenon, for which the inhomogeneous distribution changes with time in the plane of a flat sample.

1. Introduction

The SR Center of Ritsumeikan University uses the synchrotron radiation emitted when electrons with an energy of 575 MeV make an orbital motion with a radius of 0.5 m in a magnetic field of 3.8 T generated by a superconducting magnet. The critical energy of the emitted light is about 840 eV, which is very effective for XAFS measurement mainly using the soft X-ray region. Although the flux is relatively low, hard X-rays over 4 keV can be obtained at the SR Center, and the XAFS measurement is possible at the K edge of the 3d transition metal element. The XAFS beamline in the hard X-ray region has existed since the start of the SR center, but only non-focused X-ray could be used, and it was practically difficult to apply the fluorescence-yield detection. The development and upgrading of the hard X-ray XAFS beamlines, BL-3, 4 and 5, since 2009 are summarized in this article. Figure 1 shows the current arrangement of those beamlines.

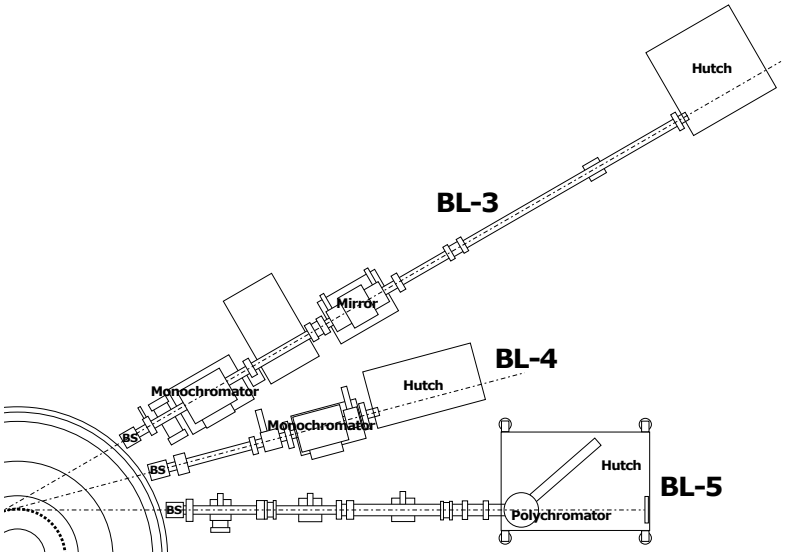

Figure 1. Hard X-ray XAFS beamlines of the SR Center.

BL-3 is a general-purpose XAFS beamline equipped with a focusing mirror and a 3-element SSD for the measurements up to 9 keV. BL-4 is a non-focusing XAFS beamline, and the imaging XAFS measurement can be performed using the built-in two-dimensional detector. BL-5 is a XAFS beamline which uses white X-rays for special purposes and is equipped with a time-resolved XAFS instrument with a dispersive X-ray optics. These three beamlines enable *in-situ* observation utilizing hard X-rays with the high transmittance and can be used for operand analysis of various functional materials. The XAFS analysis of all elements contained in the target material is possible in principle in combination with the soft X-ray XAFS beamlines in the SR center.

The electron beam size of the light source is relatively large, *ca.* 1.3 mm (horizontal) x

ca. 0.14 mm (vertical), and it is thus difficult to obtain highly brilliant X-ray with the small size. However, a compact radiation facility which can obtain X-rays from about 40 eV to about 10 keV with the practical photon flux can flexibly respond to changes in the beamline and the measurement mode.

2. BL-3

BL-3 was upgraded in 2010 as a XAFS beamline which uses focused hard X-rays.[1] As shown in Fig. 2, the beamline consists of a Golovchenko-Type double crystal monochromator,[2] a Pt-coated focusing mirror, and an experimental hutch, in which an incident slit, two ion chambers, 3-element SSD and standard sample stage are installed. X-rays are focused to the size of 4 mm (horizontal) x 2 mm (vertical) by a toroidal mirror. The glancing angle of the focusing mirror is designed as 8.73 mrad, and the cut off energy of the focused X-ray is 9.1 keV. The observed photon flux is shown in Fig. 3 by comparing with those of hard X-ray XAFS beamlines at Photon Factory (KEK). The X-ray intensity at 7 keV or higher is more than 3 orders of magnitude lower than those of the focused XAFS beamlines of Photon Factory, but in the energy range lower than 5 keV, the comparable intensity can be obtained as the non-focused beamlines of Photon Factory.

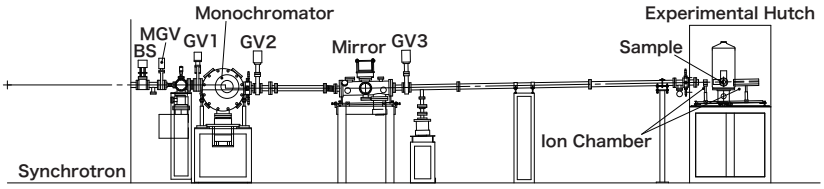

Figure 2. Schematic illustration of BL-3.

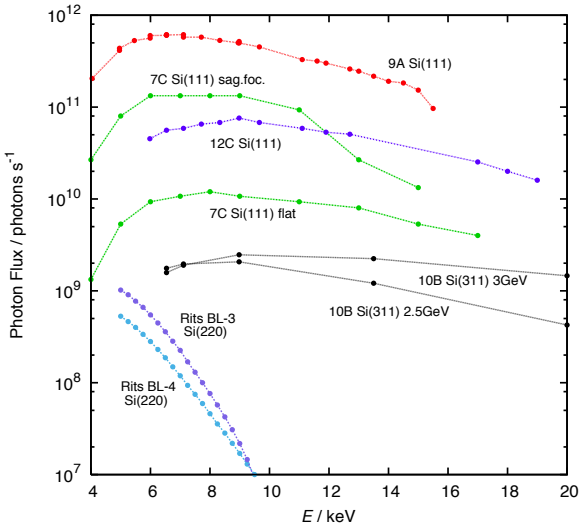

Figure 3. Photon flux of BL-3 and BL-4 compared with those of hard X-ray XAFS beamlines at Photon Factory.[2]

At BL-3, we have developed some observation cells for the *in-situ* XAFS measurements in various environments as shown in Fig. 4. It is possible to measure the XAFS spectra by the transmission mode (Fig. 4(a)) or the fluorescence yield mode (Fig. 4(b))[3] of the sample placed under the reaction gas stream at an elevated temperature up to about 900 °C. This is an effective method for analyzing the chemical state of active species during the preparation process and the reaction process of heterogeneous catalysts. Although the reaction gas is

limited, the XAFS measurements by the converted electron yield mode (Fig. 4(c)) is also possible under heating conditions.[4,5] It is also possible to perform *in-situ* XAFS measurements during the charge/discharge process of the battery materials by developing an electrochemical cell (Fig. 4(d)).[6]

The standard monochromator crystal of BL-3 is Si(220), and X-rays of 3.5 keV or higher can be used. The XAFS measurement from K to Cu at the K edge and from Cd to Yb at the L_3 edge are possible at BL-3. The capability of *in-situ* XAFS measurement is particularly useful for the chemical state analysis of many functional materials.

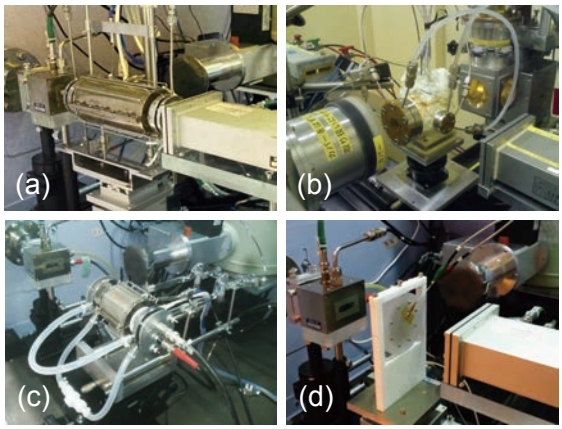

Figure 4. Observation cell for *in-situ* XAFS measurement by the transmission mode (a), the fluorescence yield mode (b), and the conversion electron yield mode (c). An electrochemical cell (d) is used for the battery materials.

4. BL-4

BL-4 shown in Fig. 5 was developed as a hard X-ray XAFS beamline since the SR Center of Ritsumeikan University opened.[7] Although the beamline control system and the X-ray detection system have been upgraded since 2009, the X-ray optics is still in use as it was constructed. Because it is possible to use X-rays without focusing, we have developed an imaging XAFS method using a two-dimensional detector. The imaging XAFS system consists of a slit, an ion chamber for the I_0 measurement, a sample stage and a two-dimensional detector, as shown in Fig. 6.

The transmitted X-ray is measured by a 2D X-ray detector, which is composed of a

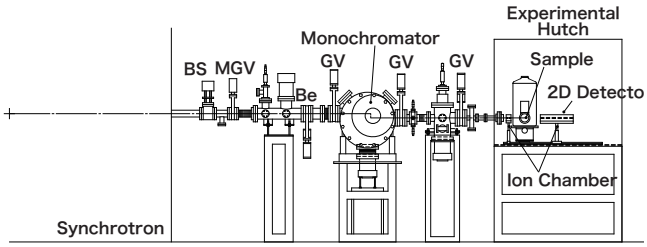

Figure 5. Schematic illustration of BL-4.

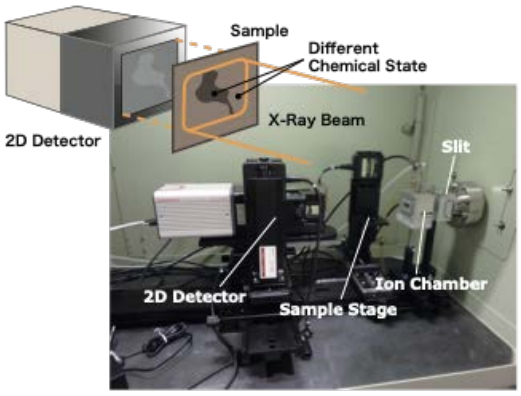

Figure 6. Imaging XAFS measurement system constructed at BL-4.

CMOS image sensor (ORCA Flash 4.0, Hamamatsu Photonics), a zooming optics of visible light and a scintillator (P43, Tb^{3+}-doped Gd_2O_2S, 10 μm thickness). The CMOS image sensor has 2048 x 2048 elements, and thus the area of *ca.* 13 mm × 13 mm is covered as the field of vision. The typical X-ray size for the imaging XAFS measurement is *ca*. 10 mm (horizontal) x 5 mm (vertical).

We have reported the inhomogeneity of the electrode reaction for the lithium iron phosphate (LFP) positive electrode used in the lithium-ion battery by means of the imaging XAFS method.[10-13] The LFP electrode material was the mixture of LFP particles as the active material, carbon particles as the conductive additive and polyvinylidene difluoride as the binder, and the LFP electrode was prepared by applying the mixture to the Al current collector sheet. The lithium ion battery (LIB) consisted of the LFP electrode, the separator sheets, the Li foil as the counter electrode and the $LiPF_6$ electrolyte solution (1 M) dissolved in the mixed solvent of ethylene carbonate and ethyl methyl carbonate. The LIB was charged or discharged to the state of charge of about 50 % and the imaging XAFS measurement was carried out at the Fe K edge. The chemical state of the Fe species was analyzed using the absorption edge energy as an index to estimate the composition of LFP (discharged state) and $FePO_4$ (charged state). A clear in-plane inhomogeneity was observed for the standard electrode (Fig. 7(a)), which was interpreted due to the low electrical conductivity of the LFP particles.[10] The imaging XAFS measurement revealed that the in-plane inhomogeneity was significantly reduced by applying a conductive coating to the surface of the Al current collector.[13] The increase of the carbon content in the LFP composite also contributed to reducing the inhomogeneity of the electrode reaction.[12] Improving the electrical conductivity of the composite electrode is important for the uniform electrode reaction, and is indispensable for the safe operation of the rechargeable battery.

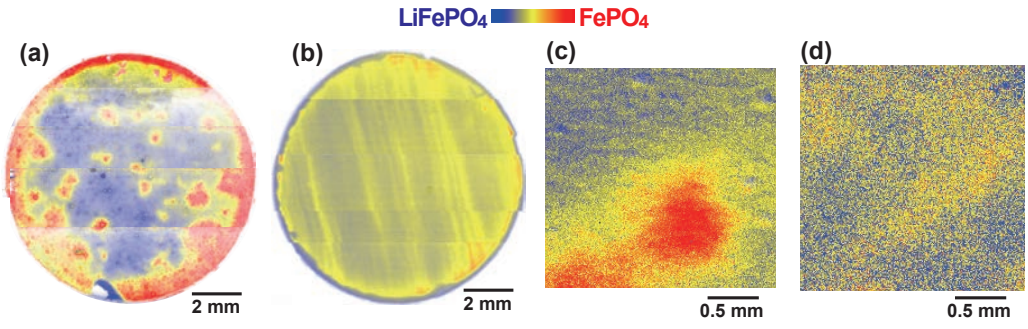

Figure 7. Chemical state map of the standard LFP electrode (a), the LFP electrode after the conductive coating on the Al collector surface (b), the LFP electrode with the carbon content of 10 wt% (c), and 20 wt% (d) without the coating during the charge/discharge process for the state of charge of about 50 %.

5. BL-5

BL-5 is a special beamline which uses white X-rays and is equipped with two kinds of time-resolved XAFS instruments with a dispersive X-ray optics. By irradiating a curved crystal with white X-rays, it is possible to simultaneously diffract X-rays in a certain energy range by utilizing the fact that the incident angle changes continuously depending on the position on the curved crystal. The diffracted X-rays in a certain energy range are focused and the sample is placed at that focal position. Thereby, the sample can be simultaneously irradiated with X-rays in the energy range required to obtain the XAFS spectrum. The X-rays which have passed through the sample are diverged again, and the XAFS spectrum can be obtained by observing with a position-sensitive detector. This is the wavelength-dispersive XAFS (DXAFS) technique, and it is known as a time-resolved XAFS measurement method because it is possible to obtain the spectrum at one time.[14)]

5.1. Two-Element Dispersive XAFS Instrument

A curved crystal is used as a polychromometer when obtaining the XAFS spectrum of the target element by the DXAFS technique. Increasing the curvature of the crystal can cover a wide energy range, in which some absorption edges are included, whereas the pixel size of the detector limits the energy resolution of the resulting XAFS spectrum. Due to the limitation of the pixel size of the position-sensitive detector and its placement location, it is necessary to use a polychromometer with an appropriate curvature for each target element to perform the DXAFS measurement with appropriate energy resolution.

A dispersive XAFS instrument, which simultaneously achieves XAFS measurements at two absorption edges using two curved crystals at the same time, has been developed at BL-5 to obtain two XANES spectra at different absorption edges, as shown in Fig. 8.[14,15)] The wide white X-ray obtained at BL-5 is divided into two parts and irradiated to two

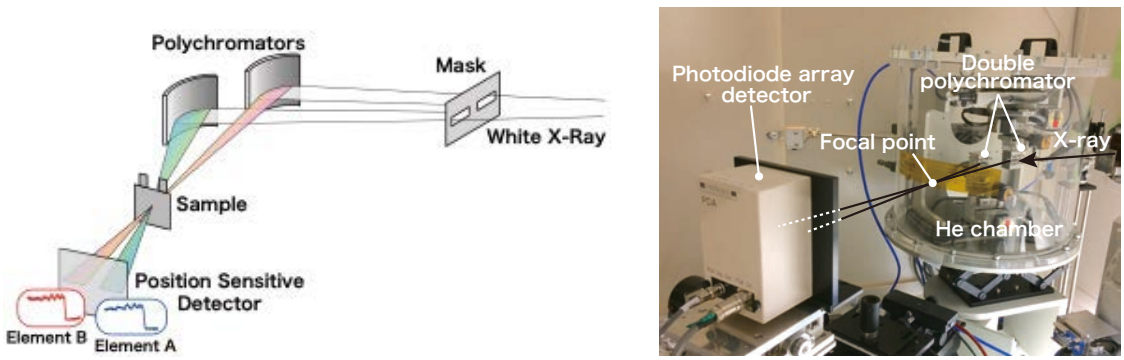

Figure 8. Concept design of two-element dispersive XAFS instrument (left) and its picture (right) developed at BL-5.

polychromometers with different curvatures. Each polychromator adjusts the Bragg angle to diffract X-rays near the absorption edge of the target element. Adjusting the relative position of two polychromators so that the diffracted light from each polychromator is focused at the same position. The sample is placed at the focal point, and the transmitted X-ray is observed by a position-sensitive detector. This instrument makes it possible to measure the XANES spectra of two elements at the same location on the sample at the same time.

Figure 9 shows the results of simultaneous observation of the K edges of Mn and Ni in the charge/discharge process of LIB using $LiMn_{1.5}Ni_{0.5}O_4$ as the positive electrode material. In the discharge process after charging to the state of $Li_{0.1}Mn_{1.5}Ni_{0.5}O_4$, the reduction from Ni^{4+} to Ni^{3+} progressed in the voltage range of around 4 V or higher, but at that time the Mn^{4+} state was maintained. The reduction of Mn^{4+} to $Mn^{3.5+}$ proceeded at the cell voltage of 2 V or less, and the Ni^{3+} state was unchanged at that time. The change in the chemical state during the charge process was completely the opposite of the discharge process. It is thus considered that the electrode reaction of Ni and Mn proceeds independently according to the cell voltage for this material.

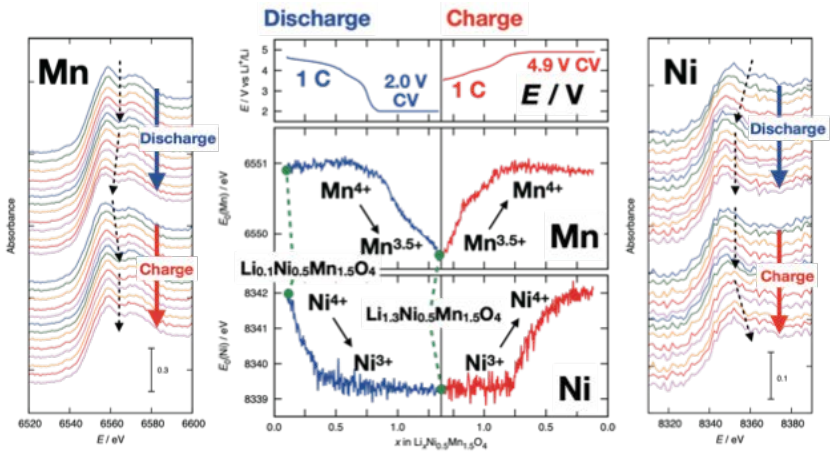

Figure 9. XANES spectral change simultaneously observed at the Mn K edge (left panel) and the Ni K edge (right panel) in the charge/discharge process of the $LiMn_{1.5}Ni_{0.5}O_4$ cathode. In the center panel, the cell voltage profile (top), the change of the edge energy at the Mn K edge (middle), and the change of the edge energy at the Ni K edge (bottom) are plotted as a function of the discharge depth.

In the inhomogeneous catalysts with multiple metal elements, it is expected that these elements will exhibit a concerted function, thus the research are being conducted on such materials using various combinations of elements. We have analyzed the reduction behavior of the Ni and Cu species in the temperature-programmed reduction (TPR) treatment to synthesize the NiCu alloy catalyst supported on SiO_2. The simultaneous XANES measurements at both the Ni and Cu K edges were performed during the TPR process for the

mixture of $Ni(NO_3)_2$ and $Cu(NO_3)_2$ hydrates supported on SiO_2, which was the precursor for the catalyst synthesis. Figure 10 shows the observed temperature changes in the XANES spectrum and the X-ray absorbance. It has been clarified that the reduction of Cu(II) to Cu(0) proceeds at the temperature range from 350 to 400 °C, and that the reduction of Ni(II) starts at the same temperature. This results suggests that the Ni(II) species is reducing triggered by the formation of Cu(0). It can be pointed out that hydrogen atoms adsorbed on Cu(0) particles may promote the reduction of the Ni(II) species.

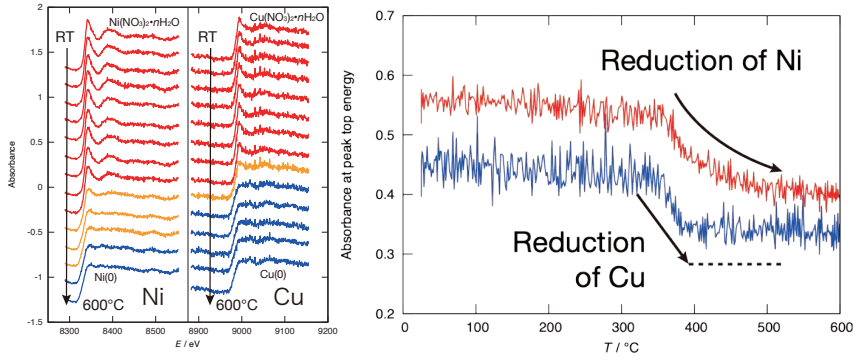

Figure 10. XANES spectral change simultaneously observed at the Ni and Cu K edges (left panel) and the absorbance change at the white line energy of the initial state as a function of temperature (left panel) during the temperature-programmed reduction process to prepare the NiCu alloy catalyst supported on SiO_2.

5.2. Vertically Dispersive XAFS Instrument

When the distribution of spatial inhomogeneity of the chemical states changes over time, the XAFS analysis is required to decompose both space and time. The general space-resolved XAFS techniques, such as the imaging XAFS technique, have extremely low time resolution due to the time required for the energy scan of X-ray. We have succeeded in developing a technique which simultaneously achieves time-resolved observations with linear spatial decomposition by combining the imaging XAFS and DXAFS techniques.

The concept design and the picture of that instrument are given in Fig. 11.[17,18] A white X-ray with a rectangular cross section is irradiated to a cylindrically curved crystal. The X-rays diffracted by the cylindrical crystal disperse the energy in the vertical direction and are focused linearly. The transmitted X-rays are diverged in the vertical direction and are detected using a two-dimensional detector. On the two-dimensional detector, the energy changes in the vertical direction, and the horizontal direction has information on different locations on the sample. Therefore, it is possible to spatially decompose the XAFS spectrum in a specific

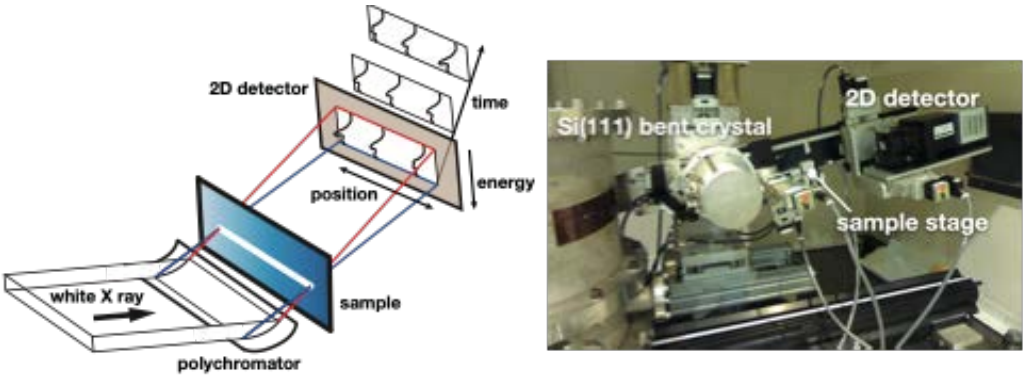

Figure 11. Concept design of vertically dispersive XAFS instrument (left) and its picture (right) developed at BL-5.

energy range on a one-dimensional line. By repeating this measurement at the desired time interval, the XAFS measurement which resolves both time and space at the same time is achieved. We named this instrument the vertically dispersive XAFS (VDXAFS) instrument.

As described above, the charge/discharge reaction of the LFP electrode proceeds heterogeneously (see Fig. 7). As a result of analysis of the electrode reaction by *in situ* imaging XAFS technique, it has been clarified that the electrode reaction proceeds preferentially at the point (reaction channel) where the conductive network is developed.[10] The electrode reaction starts from the reaction channel and spreads to the surrounding area. We observed the dynamic behavior of propagation of the electrode reaction using the VDXAFS instrument. Figure 12 shows the propagation of the chemical state change obtained on a one-dimensional line, and this linear propagation was successfully simulated using diffusion-like constants.19) This result is important information for improving the electrode configuration for suppressing the heterogeneity of the electrode reaction.

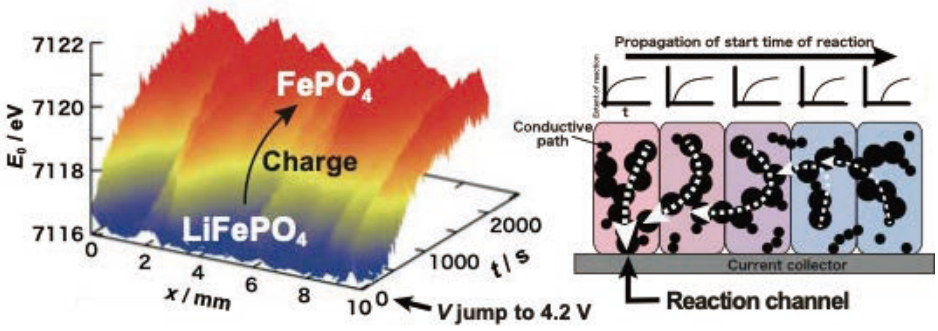

Figure 12. Reaction propagation of LFP electrode measured by the VDXAFS instrument.

6. Conclusion

Because the critical energy of the light source is about 840 eV, the flux in the hard X-ray

region is not so high, and thus the measurement of hard X-ray XAFS is disadvantageous compared to other facilities. However, taking advantage of the high mobility of the small synchrotron radiation facility, the SR Center of Ritsumeikan University, we are developing new instruments based on needs and new ideas. Various *in-situ* observation cells were developed for the purpose of embodying the needs in material evaluation. Information obtained from the chemical state analysis in a preparing or operating environment clarifies the principle of its function and presents a guiding principle for the creation of materials with higher functions. The imaging XAFS technique is useful for analyzing the in-plain inhomogeneous reaction distribution for a flat sample, although X-rays need to pass through the sample. Both the two-element DXAFS instrument and the VDXAFS instrument use the DXAFS optics, and it is possible to observe the time change of the two elements in the former and of the spatial inhomogeneity in the latter. It is possible to develop tailor-made XAFS technique which can contribute to material development at the SR Center of Ritsumeikan University.

Acknowledgement

The development of the imaging XAFS instrument, the two-element dispersive XAFS instrument and the vertically dispersive XAFS instrument was funded by New Energy and Industrial Technology Development Organization (NEDO), Research & Development Initiative for Scientific Innovation on New Generation Batteries (RISING) and Research & Development Initiative for Scientific Innovation of New Generation Batteries 2 (RISING2) projects.

References

[1] M. Katayama, K. Ozutsumi and Y. Inada, *Memoirs of the SR Center Ritsumeikan University*, **2011**, *13*, 173.

[2] M. Katayama and Y. Inada, *Memoirs of the SR Center Ritsumeikan University*, **2019**, *21*, 27.

[3] A. Suzuki, S. Yamashita, K. Furusato, M. Katayama and Y. Inada, *Memoirs of the SR Center Ritsumeikan University*, **2014**, *16*, 137.

[4] T. Watanabe, K. Ikeda, M. Katayama and Y. Inada, *J. Phys. Conf. Ser.*, **2016**, *712*, 012073.

[5] T. Watanabe, M. Katayama and Y. Inada, *Photon Factory Activity Report*, **2015**, *32*, 104.

[6] R. Miyahara, K. Hayashi, M. Katayama and Y. Inada, *Memoirs of the SR Center Ritsumeikan University*, **2013**, *15*, 35.

[7] K. Ozutsumi and K. Handa, *Rev. Sci. Instrum.*, **2004**, *75*, 111.

[8] K. Sumiwaka, M. Katayama and Y. Inada, *Memoirs of the SR Center Ritsumeikan*

University, **2012**, *14*, 11.

[9] M. Katayama, K. Sumiwaka, K. Hayashi, K. Ozutsumi, T. Ohta and Y. Inada, *J. Synchrotron Rad.*, **2012**, *19*, 717.

[10] M. Katayama, K. Sumiwaka, R. Miyahara, H. Yamashige, H. Arai, Y. Uchimoto, T. Ohta, Y. Inada and Z. Ogumi, *J. Power Sources*, **2014**, *269*, 994.

[11] Y. Orikasa, Y. Gogyo, H. Yamashige, M. Katayama, K. Chen, T. Mori, K. Yamamoto, T. Masese, Y. Inada, T. Ohta, Z. Siroma, S. Kato, H. Kinoshita, H. Arai, Z. Ogumi and Y. Uchimoto, *Sci. Rep.*, **2016**, *6*, 26382.

[12] M. Katayama, T. Nishikawa, H. Yamagishi, S. Yasuda, T. Sano, T. Kameyama, Y. Orikasa and Y. Inada, *J. Power Sources*, **2021**, *506*, 230256.

[13] T. Sano, R. Miyahara, M. Katayama, Y. Kobayashi, Y. Horiuchi, Y. Shibano and Y. Inada, *Memoirs of the SR Center Ritsumeikan University*, **2016**, *18*, 109.

[14] Y. Inada, A. Suzuki, Y. Niwa and M. Nomura, *AIP Conf. Proc.*, **2006**, *879*, 1230.

[15] M. Katayama, H. Yamagishi, Y. Yamamoto and Y. Inada, *Anal. Sci.*, **2020**, *36*, 47.

[16] M. Katayama, H. Yamagishi and Y. Inada, *Memoirs of the SR Center Ritsumeikan University*, **2017**, *19*, 33.

[17] M. Katayama, R. Miyahara, T. Watanabe, H. Yamagishi, S. Yamashita, T. Kizaki, T. Sugawara and Y. Inada, *J. Synchrotron Radiat.*, **2015**, *22*, 1227.

[18] R. Miyahara, T. Watanabe, H. Yamagishi, M. Katayama and Y. Inada, *Memoirs of the SR Center Ritsumeikan University*, **2015**, *17*, 51.

[19] H. Yamagishi, R. Miyahara, M. Katayama and Y. Inada, *Memoirs of the SR Center Ritsumeikan University*, **2017**, *19*, 25.